Generation of a coherent second-harmonic beam from incoherent conical beams

P. Stanislovaitis, A. Narmontas, V. Pyragaite,* and V. Smilgevičius
Department of Quantum Electronics, Vilnius University, Saulėtekio Avenue 9, Building 3, LT-10222 Vilnius, Lithuania
(Received 3 February 2014; published 14 April 2014)

Second-harmonic generation from incoherent conical beams is investigated. A theoretical description of an incoherent conical beam is provided. It is demonstrated that in the case of noncollinear phase matching, the spectrum of the second-harmonic beam narrows with the propagation in a nonlinear crystal. A simplified experiment with two intersecting fundamental beams is described. Numerical simulations of the nonlinear coupling equations are performed and good agreement with the theory is obtained.

DOI: 10.1103/PhysRevA.89.043821 PACS number(s): 42.25.Kb, 42.65.Ky

I. INTRODUCTION

In recent years the possibilities to generate a coherent wave from an incoherent one by means of three-wave interaction in a nonlinear crystal were investigated. Temporal [1–4], spatial [5], and both [6–8] coherences are under discussion. Experiments of optical parametric generation [1,3], oscillation [2], amplification [4,5], and second-harmonic generation (SHG) [7,8] were proposed and performed.

Here we focus on the improvement of the spatial coherence by the means of SHG. In Ref. [8] it was demonstrated that the frequency spectrum of the second-harmonic (SH) wave narrows with the propagation in a nonlinear crystal due to the temporal walk off between the fundamental and SH waves. One could try to make use of the spatial walk off in the case of the spatial beams. However, there are two transverse coordinates (x,y), while the walk off can improve the coherence only in one direction. The solution of the problem is the implementation of a conical beam, where wave vectors lie on the cone surface and the spectrum is a ring. The spatial walk off in all directions is provided by the noncollinearity. In this article we demonstrate the possibility to obtain a narrow-band SH beam from incoherent conical beams.

Coherent conical beams (Bessel beams) were introduced by Durnin [9]. Nonlinear optics of Bessel beams [10] is an interesting research area. The experiment of optical parametric generation by an incoherent conical pump revealed the possibility to generate a coherent signal when the incoherence of the pump is carried away by the idler beam [11]. The theoretical model of the incoherent conical beam was not provided yet. In this article, we describe the incoherent conical beam as a superposition of intersecting incoherent beams.

The rest of the paper is organized as follows. We start (Sec. II) from the description of the simplified experiment of noncollinear SHG. In Sec. III, we provide the theoretical model of incoherent conical beams, and we describe SHG in the case of an incoherent conical pump. The special case of two intersecting beams is described too. In Sec. IV, the numerical simulation of nonlinear coupling equations is performed. Finally, conclusions are drawn in Sec. V.

*viktorija.pyragaite@ff.vu.lt

II. EXPERIMENTAL

First, we describe the experiment in which two intersecting fundamental beams generate a SH beam. The first fundamental beam is spatially incoherent and the second one is a coherent beam.

The experimental setup is presented in Fig. 1. We used two temporally coherent laser sources. Each source had the same characteristics: 2.2 mJ pulse energy, 1 kHz frequency, 1064 nm wavelength, pulse duration approximately 75 ps. Both sources radiate spatially coherent beams. In order to get a spatially incoherent beam, in one of the laser beams we put phase distortion film. The width of the coherent beam at FWHM was 1.6 mm on the x axis and 1.2 mm on the y axis. The angle between intersecting beams was 18° (approximately 12° in crystal). For SH generation we used 2 cm long KDP Type-I phase matching crystal. The coherent and incoherent beams were intersected in the yz plane, while the crystal was positioned in such orientation that the walk off effect occurred in the perpendicular plane (xz). To separate the fundamental and second-harmonic output beams we used an iris aperture. Also in order to register the intensity distribution and angular spectra of SH beam with CCD we used neutral filters to reduce radiation intensity. We registered generated noncollinear SH intensity distribution in the crystal output plane by using a 2f-2f imaging technique. The lens with 250 mm focal length was used. We put the lens 500 mm from the crystal output plane and put a CCD camera 500 mm from lens. To register SH angular spectra we used an f-f imaging technique. In this case we used a lens with 500 mm focal length.

The angular spectra of the input fundamental beams as well as the output second-harmonic beam are depicted in Fig. 2. Here $\theta_{x,y}^{\mathrm{out}}$ denotes the angles outside the crystal. The beams were intersected in the yz plane and the walk off takes place in the xz plane. As we can see, the second-harmonic spectrum can be fitted by the theoretical line, Eq. (46). In this case, the spectral width decreases only in one direction. The direction of the line depends on the ratio of the intersection angle of the fundamental beams to the walk-off angle. The line can be rotated by changing the intersection plane of the fundamental beams, see bottom right of Fig. 2. The question may arise: what will be the angular spectrum of the second-harmonic beam when two conical beams interact, one consisting of the incoherent beams placed on a ring and the second consisting of the narrow-band coherent beams? In this case the direction

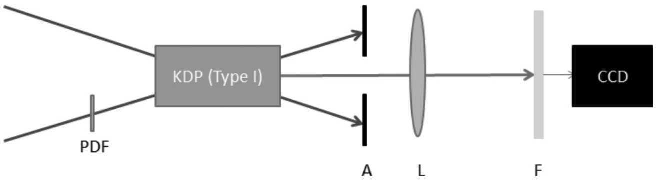

FIG. 1. Experimental setup. PDF: phase distortion film; A: aperture, L: lens; F: neutral filter.

of the line is undefined and as we will see from the below theoretical consideration, the spectrum of the second harmonic is a narrow-band central spot. In other words, the conical configuration forces the decrease of the spectral width in all directions.

III. THEORETICAL

Now we will describe the model of the incoherent conical beam. It is generated from a large amount of intersecting uncorrelated beams. Next, the second-harmonic generation from two incoherent conical beams will be discussed.

A. Incoherent conical beam model

We assume N incoherent beams, the spectra of which are placed on the ring. Then the complex amplitude of the composed conical beam reads

$$A(x,y) = \sum_{n=1}^{N} B_n(x,y) \exp[i\beta_0 \cos(\varphi_n)x + i\beta_0 \sin(\varphi_n)y], \tag{1}$$

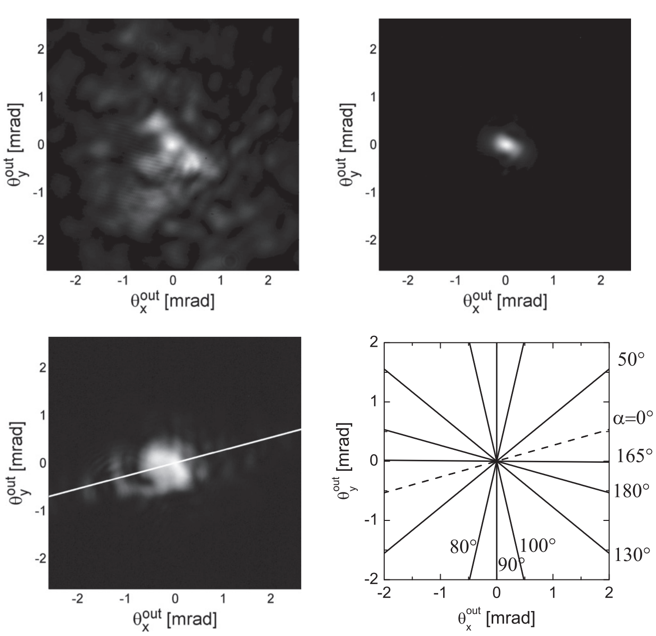

FIG. 2. Experimental angular spectra of the first (top left) and second (top right) fundamental beams as well as generated second-harmonic beam (bottom left). White line: Eq. (46). Bottom right: spectral lines for intersection planes rotated by the angle α with respect to yz plane, Eq. (48).

where $\varphi_n = 2\pi(n-1)/N$ and B_n are the propagation angle and complex amplitude of the nth beam, respectively. $\beta_0 = k_0\theta_0$, where k_0 and $2\theta_0$ are the wave number of the fundamental beam and cone angle, respectively. x, y are the transverse Cartesian coordinates. Further we turn to cylindrical coordinates r, φ: $x = r\cos\varphi$, $y = r\sin\varphi$. Then the complex amplitude can be written as

$$A(r,\varphi) = \sum_{n=1}^{N} B_n(r,\varphi) \exp[i\beta_0 r \cos(\varphi_n - \varphi)]. \tag{2}$$

Let us define the spectral amplitude as

$$S(\beta_x,\beta_y) = \int_{-\infty}^{\infty}\int_{-\infty}^{\infty} A(x,y)\exp(-i\beta_x x - i\beta_y y)dxdy \tag{3}$$

or in cylindrical coordinates:

$$S(\beta,\theta) = \int_0^{\infty}\int_0^{2\pi} A(r,\varphi)\exp[-i\beta r\cos(\theta-\varphi)]rdrd\varphi. \tag{4}$$

Here $\beta_x = \beta\cos\theta$, $\beta_y = \beta\sin\theta$. By the use of Jacobi-Anger expansion:

$$\exp(iq\cos\theta) = \sum_{k=-\infty}^{\infty} i^k J_k(q)\exp(ik\theta), \tag{5}$$

where $J_k(q)$ is a Bessel function, we obtain

$$S(\beta,\theta) = \sum_{n=1}^{N}\sum_{k=-\infty}^{\infty}\sum_{l=-\infty}^{\infty}\int_0^{2\pi}\int_0^{\infty} rdrd\varphi i^{-k+l} B_n(r,\varphi) \times J_k(\beta r)J_l(\beta_0 r)\exp\left[-ik(\theta-\varphi) + il(\varphi_n - \varphi)\right]. \tag{6}$$

Further we will calculate the average $\langle S^*(\beta',\theta')S(\beta,\theta)\rangle$. We need to know the correlation functions $\langle B_{n'}^*(x',y')B_n(x,y)\rangle$. We assume that the correlation radius of all intersecting beams is the same and the correlation functions are Gaussian. The beams are not correlated with each other. In this theoretical treatment we assume that the beams are homogeneous. In Cartesian coordinates, the correlation function can be written as

$$\langle B_{n'}^*(x',y')B_n(x,y)\rangle = b_0^2\delta_{nn'}\exp\left(-\frac{(x-x')^2}{\rho^2} - \frac{(y-y')^2}{\rho^2}\right), \tag{7}$$

where b_0 is an amplitude and ρ is a correlation radius. $\delta_{nn'}$ is the Kronecker δ. In cylindrical coordinates one obtains

$$\langle B_{n'}^*(r',\varphi')B_n(r,\varphi)\rangle = b_0^2\delta_{nn'}\exp\left(-\frac{1}{\rho^2}[r^2 + r'^2 - 2rr'\cos(\varphi-\varphi')]\right). \tag{8}$$

Further we make use of the relation [12]

$$\exp[q\cos(\theta)] = \sum_{p=-\infty}^{\infty} I_p(q)\exp(ip\theta), \tag{9}$$

where $I_p(q)$ is a modified Bessel function. By the use of Eqs. (6), (8), and (9) we obtain

$$\langle S^*(\beta',\theta')S(\beta,\theta)\rangle = b_0^2\sum_{n=1}^{N}\sum_{p=-\infty}^{\infty}\sum_{k,k'=-\infty}^{\infty}\sum_{l,l'=-\infty}^{\infty} i^{-k+l+k'-l'}\exp\left[-ik\theta+ik'\theta'+i(l-l')\varphi_n\right]\int_0^{2\pi}\int_0^{\infty}\int_0^{2\pi}\int_0^{\infty} d\varphi dr d\varphi' dr' rr'$$
$$\times\exp\left[-i(l-k)\varphi+i(l'-k')\varphi'+ip(\varphi-\varphi')\right]J_k(\beta r)J_l(\beta_0 r)J_{k'}(\beta' r')J_{l'}(\beta_0 r')I_p(2rr'/\rho^2)$$
$$\times\exp(-r^2/\rho^2)\exp(-r'^2/\rho^2). \quad (10)$$

Now we are able to integrate over azimuthal angles φ and φ'. We obtain

$$\langle S^*(\beta',\theta')S(\beta,\theta)\rangle = b_0^2(2\pi)^2\sum_{n=1}^{N}\sum_{p=-\infty}^{\infty}\sum_{k,k'=-\infty}^{\infty}\exp[-ik(\theta-\varphi_n)+ik'(\theta'-\varphi_n)]$$
$$\times\int_0^{\infty}\int_0^{\infty} drdr'rr'J_k(\beta r)J_{p+k}(\beta_0 r)J_{k'}(\beta' r')J_{k'+p}(\beta_0 r')I_p(2rr'/\rho^2)\exp(-r^2/\rho^2)\exp(-r'^2/\rho^2). \quad (11)$$

Further we make use of the summation formula [12]:

$$\exp(ip\psi)J_p(Rr) = \sum_{k=-\infty}^{\infty}J_k(\beta r)J_{k+p}(\beta_0 r)\exp[ik(\varphi_n-\theta)], \quad (12)$$

where

$$R^2 = \beta^2+\beta_0^2-2\beta\beta_0\cos(\varphi_n-\theta) \quad \text{and} \quad \exp(i2\psi) = \frac{\beta_0-\beta\exp[-i(\varphi_n-\theta)]}{\beta_0-\beta\exp[i(\varphi_n-\theta)]}. \quad (13)$$

So, the summations over k and k' give

$$\langle S^*(\beta',\theta')S(\beta,\theta)\rangle = b_0^2(2\pi)^2\sum_{n=1}^{N}\sum_{p=-\infty}^{\infty}\exp[ip(\psi-\psi')]\int_0^{\infty}\int_0^{\infty} drdr'rr'$$
$$\times J_p(Rr)J_p(R'r')I_p(2rr'/\rho^2)\exp(-r^2/\rho^2)\exp(-r'^2/\rho^2), \quad (14)$$

where R' and ψ' are obtained from Eqs. (13) by replacing β, θ with β', θ'. We integrate over r' by use of the relation [12]:

$$\int_0^{\infty} v\exp(-v^2/\rho^2)I_p(\gamma_1 v)J_p(\gamma_2 v)dv = \frac{\rho^2}{2}\exp\left(\frac{\gamma_1^2-\gamma_2^2}{4}\rho^2\right)J_p(\gamma_1\gamma_2\rho^2/2). \quad (15)$$

So,

$$\langle S^*(\beta',\theta')S(\beta,\theta)\rangle = b_0^2\rho^2(2\pi)^2\frac{1}{2}\sum_{n=1}^{N}\sum_{p=-\infty}^{\infty}\exp[ip(\psi-\psi')]\exp\left(-\frac{R'^2\rho^2}{4}\right)\int_0^{\infty} rJ_p(Rr)J_p(R'r)dr. \quad (16)$$

By the use of the relation

$$\int_0^{\infty} rJ_p(Rr)J_p(R'r)dr = \frac{\delta(R-R')}{R} \quad (17)$$

we can integrate over r:

$$\langle S^*(\beta',\theta')S(\beta,\theta)\rangle = b_0^2\rho^2(2\pi)^2\frac{1}{2}\sum_{n=1}^{N}\sum_{p=-\infty}^{\infty}\exp[ip(\psi-\psi')]\exp\left(-\frac{R^2\rho^2}{4}\right)\frac{\delta(R-R')}{R}. \quad (18)$$

Here $\delta(\dots)$ is a Dirac δ function. The sum over p also can be calculated:

$$\langle S^*(\beta',\theta')S(\beta,\theta)\rangle = \frac{b_0^2}{2}\rho^2(2\pi)^3\sum_{n=1}^{N}\exp\left(-\frac{R^2\rho^2}{4}\right)$$
$$\times\frac{\delta(R-R')}{R}\delta(\psi-\psi'). \quad (19)$$

Since the Jacobian

$$\left|\frac{\partial R}{\partial\beta}\frac{\partial\psi}{\partial\theta}-\frac{\partial R}{\partial\theta}\frac{\partial\psi}{\partial\beta}\right| = \frac{\beta}{R}, \quad (20)$$

we can write

$$\langle S^*(\beta',\theta')S(\beta,\theta)\rangle = \frac{b_0^2}{2}\rho^2(2\pi)^3\times\sum_{n=1}^{N}\exp\left(-\frac{R^2\rho^2}{4}\right)$$
$$\times\frac{\delta(\beta-\beta')}{\beta}\delta(\theta-\theta'). \quad (21)$$

Here summation over n is due to R, see Eq. (13). In the case of a large amount of beams N, the sum over n can be replaced by the integral: $\sum_{n=1}^{N}\to\frac{N}{2\pi}\int_0^{2\pi}d\varphi_n$. By the use of Eqs. (13)

and (9) we obtain the following spectral intensity:

$$G(\beta,\theta) = \frac{N}{2\pi} b_0^2 \frac{4}{\Delta\beta^2} 2\pi^2 \exp\left(- \frac{\beta^2 + \beta_0^2}{\Delta\beta^2} \right) I_0\left(\frac{2\beta\beta_0}{\Delta\beta^2} \right), \tag{22}$$

where ρ was replaced by $2/\Delta\beta$, $\Delta\beta$ is a spectral radius. Here the spectral intensity G is defined as

$$\langle S^*(\beta',\theta')S(\beta,\theta)\rangle = (2\pi)^2 G(\beta,\theta) \frac{\delta(\beta - \beta')}{\beta} \delta(\theta - \theta') \tag{23}$$

or in Cartesian coordinates

$$\langle S^*(\beta_x',\beta_y')S(\beta_x,\beta_y)\rangle = (2\pi)^2 G(\beta_x,\beta_y)\delta(\beta_x - \beta_x')\delta(\beta_y - \beta_y'). \tag{24}$$

Finally, Eq. (22) can be simplified by assuming that the cone angle is much larger than the spectral width: $\beta_0 \gg \Delta\beta$. Then $I_0(\xi) \approx \exp(\xi)/\sqrt{2\pi\xi}$ and at $\xi \approx 2\beta_0^2/\Delta\beta^2$ ($\beta \approx \beta_0$):

$$G(\beta,\theta) = N b_0^2 \frac{2\sqrt{\pi}}{\Delta\beta\beta_0} \exp\left(- \frac{(\beta - \beta_0)^2}{\Delta\beta^2} \right). \tag{25}$$

In the limit $\Delta\beta \to 0$ we have

$$G(\beta,\theta) = N b_0^2 \frac{2\pi}{\beta_0} \delta(\beta - \beta_0). \tag{26}$$

So, we have obtained simple expressions (25) and (26) for incoherent conical beams, which consist of uncorrelated incoherent and coherent beams, respectively.

B. Nonlinear coupling equations

Let us discuss the equations of three-wave interaction, which are given by:

$$\begin{aligned}
&\frac{\partial A_1}{\partial z} + \frac{i}{2k_{10}} \left(\frac{\partial^2 A_1}{\partial x^2} + \frac{\partial^2 A_1}{\partial y^2} \right) = -\sigma A_2^* A_3 \exp(i\Delta k z),\\
&\frac{\partial A_2}{\partial z} + \frac{i}{2k_{20}} \left(\frac{\partial^2 A_2}{\partial x^2} + \frac{\partial^2 A_2}{\partial y^2} \right) = -\sigma A_1^* A_3 \exp(i\Delta k z),\\
&\frac{\partial A_3}{\partial z} + \frac{i}{2k_{30}} \left(\frac{\partial^2 A_3}{\partial x^2} + \frac{\partial^2 A_3}{\partial y^2} \right) + \gamma \frac{\partial A_3}{\partial x}\\
&\quad = 2\sigma A_1 A_2 \exp(-i\Delta k z).
\end{aligned} \tag{27}$$

A Type-I interaction is assumed. A_j are complex amplitudes of fundamental ($j = 1,2$) and second-harmonic ($j = 3$) beams. $k_{j0}, \gamma, \Delta k, \sigma$ are the wave number, a walk-off angle, the phase mismatch, and the nonlinear coupling coefficient, respectively. As in the experiment the walk off takes place in the xz plane. In the case of second-harmonic generation we have $k_{10} = k_{20} = k_0$, $k_{30} = 2k_0$. Further we assume that pump depletion is weak and the right-hand terms in the first two equations are negligible. Then for the spectral amplitudes one obtains

$$\begin{aligned}
\frac{\partial S_1}{\partial z} &= i \frac{\beta_x^2 + \beta_y^2}{2k_0} S_1,\\
\frac{\partial S_2}{\partial z} &= i \frac{\beta_x^2 + \beta_y^2}{2k_0} S_2,\\
\frac{\partial S_3}{\partial z} &= i \frac{\beta_x^2 + \beta_y^2}{2k_{30}} S_3 - i\gamma\beta_x S_3 + \frac{2\sigma}{4\pi^2} \exp(-i\Delta k z) \int_{-\infty}^{\infty}\int_{-\infty}^{\infty} d\beta_{x1} d\beta_{y1} S_1(\beta_x - \beta_{x1},\beta_y - \beta_{y1}) S_2(\beta_{x1},\beta_{y1}).
\end{aligned} \tag{28}$$

Solutions of the equations are the following

$$\begin{aligned}
S_1 &= S_{10}(\beta_x,\beta_y) \exp\left[\frac{i}{2k_0} (\beta_x^2 + \beta_y^2) z \right],\\
S_2 &= S_{20}(\beta_x,\beta_y) \exp\left[\frac{i}{2k_0} (\beta_x^2 + \beta_y^2) z \right],\\
S_3(\beta_x,\beta_y,z) &= \frac{2\sigma}{4\pi^2} \exp\left(i \frac{\beta_x^2 + \beta_y^2}{2k_{30}} z - i\gamma\beta_x z \right) \int_0^z dz' \exp\left(-i\Delta k z' - i \frac{\beta_x^2 + \beta_y^2}{2k_{30}} z' + i\gamma\beta_x z' \right)\\
&\quad \times \int_{-\infty}^{\infty}\int_{-\infty}^{\infty} d\beta_{x1} d\beta_{y1} S_1(\beta_x - \beta_{x1},\beta_y - \beta_{y1},z') S_2(\beta_{x1},\beta_{y1},z'),
\end{aligned} \tag{29}$$

where S_{10} and S_{20} are the spectral amplitudes of the input fundamental beams (at $z = 0$). Insertion of the first two equations of Eqs. (29) into the third equation and integration over z' yield

$$\begin{aligned}
S_3(\beta_x,\beta_y,z) &= \frac{2\sigma z}{4\pi^2} \exp\left(i \frac{\beta_x^2 + \beta_y^2}{2k_{30}} z - i\gamma\beta_x z \right) \int_{-\infty}^{\infty}\int_{-\infty}^{\infty} d\beta_{x1} d\beta_{y1}\\
&\quad \times \exp\left(\frac{i a(\beta_{x1},\beta_{y1},\beta_x,\beta_y) z}{2} \right) \operatorname{sinc} \frac{a(\beta_{x1},\beta_{y1},\beta_x,\beta_y) z}{2} S_{10}(\beta_x - \beta_{x1},\beta_y - \beta_{y1}) S_{20}(\beta_{x1},\beta_{y1}).
\end{aligned} \tag{30}$$

Here

$$a(\beta_{x1},\beta_{y1},\beta_x,\beta_y) = -\Delta k - \frac{\beta_x^2 + \beta_y^2}{2k_{30}} + \beta_x\gamma + \frac{(\beta_x - \beta_{x1})^2 + (\beta_y - \beta_{y1})^2}{2k_0} + \frac{\beta_{x1}^2 + \beta_{y1}^2}{2k_0}. \tag{31}$$

Now we will find the expression of the spectral intensity of the second-harmonic beam. The average

$$\langle S_3(\beta_x,\beta_y,z)S_3^*(\beta_x',\beta_y',z)\rangle = \frac{z^2 4\sigma^2}{16\pi^4}\int_{-\infty}^{\infty}\int_{-\infty}^{\infty}\int_{-\infty}^{\infty}\int_{-\infty}^{\infty} d\beta_{x1}d\beta_{y1}d\beta_{x2}d\beta_{y2}\text{sinc}\frac{a_1 z}{2}\text{sinc}\frac{a_2 z}{2} \times \langle S_{10}(\beta_x-\beta_{x1},\beta_y-\beta_{y1})S_{20}(\beta_{x1},\beta_{y1})S_{10}^*(\beta_x'-\beta_{x2},\beta_y'-\beta_{y2})S_{20}^*(\beta_{x2},\beta_{y2})\rangle. \tag{32}$$

Here $a_1 = a(\beta_{x1},\beta_{y1},\beta_x,\beta_y)$ and $a_2 = a(\beta_{x2},\beta_{y2},\beta_x',\beta_y')$. We calculate the average of the fourth-order moment assuming that the fundamental beams are Gaussian processes. The beams are assumed to be homogeneous and uncorrelated. Then the fourth-order moment can be factorized into second-order moments and by the use of Eq. (24) we obtain:

$$\langle S_{10}(\beta_x-\beta_{x1},\beta_y-\beta_{y1})S_{20}(\beta_{x1},\beta_{y1})S_{10}^*(\beta_x'-\beta_{x2},\beta_y'-\beta_{y2})S_{20}^*(\beta_{x2},\beta_{y2})\rangle$$
$$= 16\pi^4 G_{10}(\beta_x-\beta_{x1},\beta_y-\beta_{y1})G_{20}(\beta_{x1},\beta_{y1})\delta(\beta_x-\beta_{x1}-\beta_x'+\beta_{x2})\delta(\beta_{x1}-\beta_{x2})\delta(\beta_y-\beta_{y1}-\beta_y'+\beta_{y2})\delta(\beta_{y1}-\beta_{y2}). \tag{33}$$

Finally, we obtain the spectral intensity of the second-harmonic beam:

$$4\pi^2 G_3(\beta_x,\beta_y) = z^2 4\sigma^2\int_{-\infty}^{\infty}\int_{-\infty}^{\infty} d\beta_{x1}d\beta_{y1}G_{10}(\beta_x-\beta_{x1},\beta_y-\beta_{y1})G_{20}(\beta_{x1},\beta_{y1})\text{sinc}^2\frac{a_1 z}{2}. \tag{34}$$

We will use this expression in the further consideration.

C. Second harmonic from two incoherent conical beams

Let us assume two fundamental conical beams, one of which is incoherent azimuthally and radially, Eq. (25). The second is assumed to be incoherent only azimuthally, Eq. (26). We call them the first and the second fundamental beams, respectively. So, we insert the following expressions of the spectral intensities of the fundamental beams into Eq. (34):

$$G_{10}(\beta_x,\beta_y) = Nb_0^2\frac{2\sqrt{\pi}}{\Delta\beta\beta_0}\exp\left(-\frac{\left(\sqrt{\beta_x^2+\beta_y^2}-\beta_0\right)^2}{\Delta\beta^2}\right),$$
$$G_{20}(\beta_x,\beta_y) = Nb_0^2\frac{2\pi}{\beta_0}\delta\left(\sqrt{\beta_x^2+\beta_y^2}-\beta_0\right). \tag{35}$$

These expressions were derived from Eqs. (25) and (26) by converting the cylindrical coordinates to Cartesian. The substitution gives

$$4\pi^2 G_3(\beta_x,\beta_y) = 4\sigma^2 z^2 N^2 b_0^4 4\pi\sqrt{\pi}\frac{1}{\Delta\beta\beta_0}\int_{-\infty}^{\infty}\int_{-\infty}^{\infty} d\beta_{x1}d\beta_{y1} \times\exp\left(-\frac{\left(\sqrt{\beta^2+\beta_1^2-2\beta\beta_1\cos(\theta-\theta_1)}-\beta_0\right)^2}{\Delta\beta^2}\right) \times\frac{\delta\Big(\beta_1-\beta_0\Big)}{\beta_1}\text{sinc}^2\left(\frac{z}{2}\Big(-\Delta k-\frac{\beta^2}{2k_{30}}+\beta_x\gamma +\frac{\beta^2+\beta_1^2-2\beta\beta_1\cos(\theta-\theta_1)}{2k_0}+\frac{\beta_1^2}{2k_0}\Big)\right), \tag{36}$$

where $\beta_{x1} = \beta_1\cos\theta_1$, $\beta_{y1} = \beta_1\sin\theta_1$. Further we return to cylindrical coordinates: $\int\int d\beta_{x1}d\beta_{y1} \to \int\int\beta_1 d\beta_1 d\theta_1$. We make use of the δ function and integrate over β_1. We obtain the following integral over θ_1:

$$G_3(\beta,\theta) = \frac{z^2}{L_n^2}N^2 b_0^2\frac{1}{\Delta\beta\beta_0}\frac{4}{\sqrt{\pi}}\int_0^{2\pi}d\theta_1 \times\exp\left(-\frac{\left(\sqrt{\beta^2+\beta_0^2-2\beta\beta_0\cos(\theta-\theta_1)}-\beta_0\right)^2}{\Delta\beta^2}\right) \times\text{sinc}^2\left[\frac{z}{2}\left(\frac{\beta^2}{4k_0}+\beta\gamma\cos\theta-\frac{\beta\beta_0\cos(\theta-\theta_1)}{k_0}\right)\right]. \tag{37}$$

Here we assumed the noncollinear phase matching:

$$\Delta k = \beta_0^2/k_0 \tag{38}$$

and used the relation $k_{30} = 2k_0$. We also introduced a nonlinear interaction length $L_n = 1/\sigma b_0$.

In Fig. 3 the calculated spectra of the generated second-harmonic beam are presented. The spectrum narrows during the propagation in the nonlinear crystal. The cone angle ($2\theta_0 =$ 62 mrad) was chosen to be comparable with the walk-off angle ($\gamma = -28$ mrad). So, its influence is sufficiently large. In the right bottom of Fig. 3 we compare the spectral widths in x and y directions. They are not the same due to the walk off. The walk off takes place in the x direction, so $\Delta\theta_x^{\text{out}}$ decreases faster than $\Delta\theta_y^{\text{out}}$.

We note that the angular structure of the SH beam generated from the incoherent conical beams differs from the structure, which was discussed in Ref. [13]. There, the coherent conical pump beam was investigated and it was shown that the spectrum of the generated SH beam can be factorized into two parts: one describing the transverse phase matching (TPM) and another arising from the longitudinal phase matching (LPM). TPM yields the spectral width of the SH equal to $2.5/(k_1 d)$, where d is the beam radius of the pump beam. LPM in our notations reads as $\beta^2/4k_0 + \gamma\beta_x = 0$. In our case, the TPM and LPM parts can not be factorized, see Eq. (37). The maximum of the expression is obtained at $\beta = 0$, so the

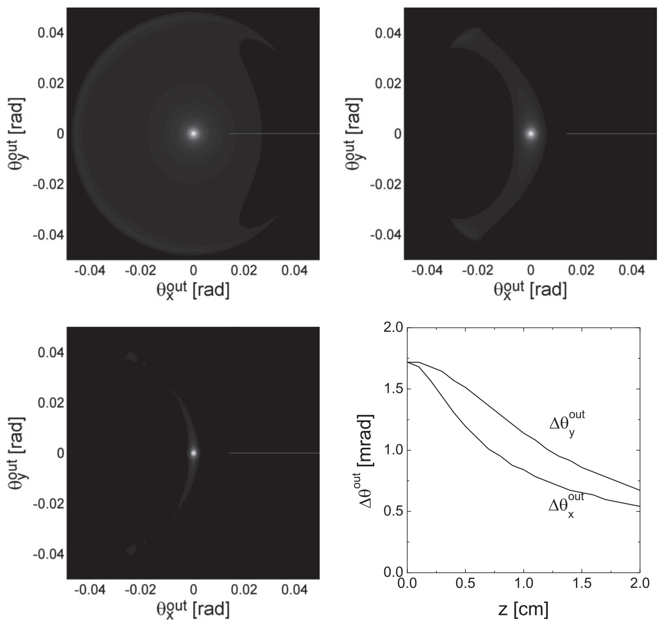

FIG. 3. Theoretically calculated spectra [Eq. (37)] of the second-harmonic beam. Bottom right: theoretically calculated spectral width of second-harmonic beam at $\theta = 0$ ($\Delta\theta_x^{out}$) and $\theta = \pi/2$ ($\Delta\theta_y^{out}$). Type-I KDP crystal, fundamental wavelength $\lambda_1 = 1.064\ \mu$m, $\theta_0^{out} = 2.7^\circ$, $\Delta\beta/k_0 = 2$ mrad, $\gamma = -28$ mrad. z: 200 μm (top left), 2 mm (top right), 1 cm (bottom left).

spectrum narrows with the propagation in a nonlinear crystal. We note that spectral width would not decrease if both pump beams were radially incoherent, Eq. (25). One of the pump beams has to be radially coherent.

From Eqs. (37) and (35) it follows for the spectral radiance:

$$\frac{G_3(0,0)}{G_{10}(\beta_0,0)} = 4N\frac{z^2}{L_n^2}. \tag{39}$$

D. Two intersecting beams

In the experiment there were only two intersecting fundamental beams, Fig. 1. In this case, from Eq. (21) we obtain the following expression for the first beam:

$$G_{10}(\beta_x,\beta_y) = \pi\frac{4}{\Delta\beta^2}b_0^2\exp\left(-\frac{\beta_x^2+(\beta_y-\beta_0)^2}{\Delta\beta^2}\right). \tag{40}$$

For the second beam we obtain

$$G_{20}(\beta_x,\beta_y) = 4\pi^2 b_0^2\delta(\beta_x)\delta(\beta_y+\beta_0). \tag{41}$$

The beams are intersected in the yz plane. The insertion of Eqs. (40) and (41) into Eq. (34) gives

$$4\pi^2 G_3(\beta_x,\beta_y,z) = 4\pi^2 z^2 4\sigma^2 b_0^2 G_{10}(\beta_x,\beta_y+\beta_0)\text{sinc}^2\frac{a_0 z}{2}, \tag{42}$$

where

$$a_0 = -\Delta k - \frac{\beta_x^2+\beta_y^2}{4k_0} + \beta_x\gamma + \frac{\beta_x^2}{2k_0} + \frac{(\beta_y+\beta_0)^2}{2k_0} + \frac{\beta_0^2}{2k_0}. \tag{43}$$

By the use of Eq. (38) we obtain

$$a_0 = \beta_x\gamma + \beta_y\frac{\beta_0}{k_0} + \frac{\beta_x^2+\beta_y^2}{4k_0}. \tag{44}$$

So, in the case of two intersecting beams, the spectral intensity of the second harmonic is

$$\frac{G_3(\beta_x,\beta_y,z)}{G_{10}(0,\beta_0)} = 4\frac{z^2}{L_n^2}\exp\left(-\frac{\beta_x^2+\beta_y^2}{\Delta\beta^2}\right) \times \text{sinc}^2\left(\frac{z}{2}\left[\beta_x\gamma + \beta_y\frac{\beta_0}{k_0} + \frac{\beta_x^2+\beta_y^2}{4k_0}\right]\right). \tag{45}$$

At large z the second-harmonic spectrum obeys maximum condition at the line described by the equation:

$$\beta_x = -\beta_y\beta_0/(k_0\gamma). \tag{46}$$

This is confirmed by the experiment, Fig. 2. For the spectral radiance we obtain:

$$\frac{G_3(0,0)}{G_{10}(\beta_0,0)} = 4\frac{z^2}{L_n^2}. \tag{47}$$

In the case of conical beams this ratio is N times larger, Eq. (39). The factor of 4 appears due to the factor of 2 in the nonlinear term of the third equation of Eqs. (27).

Equation (46) can generalized for the case when the intersection plane of the fundamental beams is rotated by angle

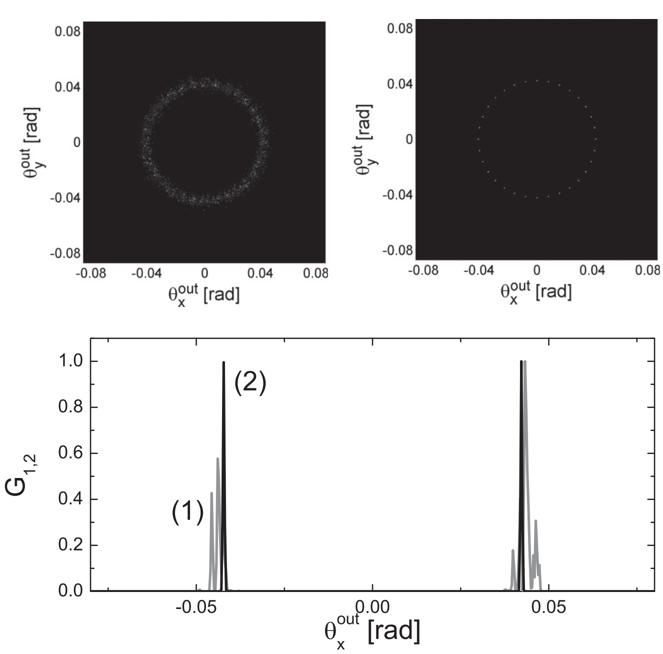

FIG. 4. Numerically calculated spectra of the first (top left) and the second (top right) fundamental beams. Bottom: normalized spectra of the first (1) and the second (2) fundamental beams at $\theta_y^{out} = 0$. Type-I KDP crystal, fundamental wavelength $\lambda_1 = 1.064\ \mu$m, $\theta_0^{out} = 2.7^\circ$, $\Delta\beta/k_0 = 2$ mrad, $d = 700\ \mu$m, $N = 32$. One simulation.

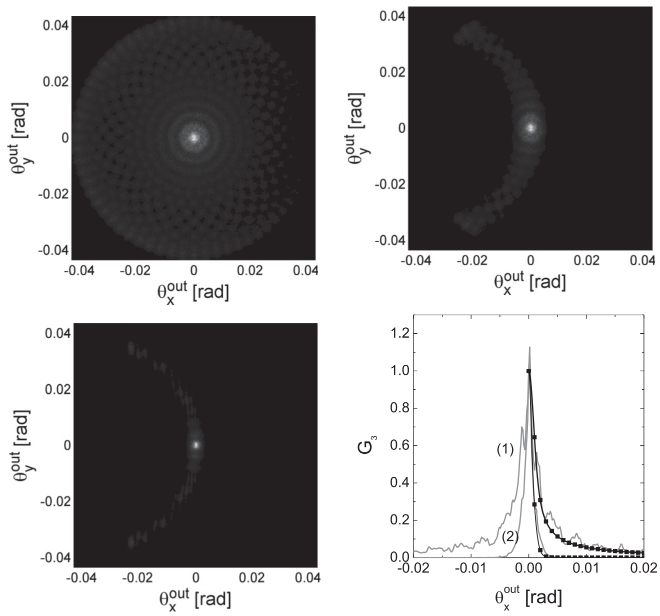

FIG. 5. Numerically calculated spectra of the second-harmonic beam. Type-I KDP crystal, fundamental wavelength $\lambda_1 = 1.064$ μm, $\theta_0^{out} = 2.7^\circ$, $\Delta\beta/k_0 = 2$ mrad, $\gamma = -28$ mrad. z: 200 μm (top left), 2 mm (top right), 1 cm (bottom left). Bottom right: numerically (gray lines) and theoretically (black lines and squares) calculated normalized spectra at $\theta_y^{out} = 0$, $z = 200$ μm (1) and $z = 1$ cm (2). $d = 700$ μm, $L_n = 20$ cm, $N = 32$, average of 50 simulations.

α. Then, the line obeys the following equation:

$$\beta_x = -\beta_y \frac{\beta_0 \cos(\alpha)/k_0}{\gamma + \beta_0 \sin(\alpha)/k_0}. \tag{48}$$

IV. NUMERICAL SIMULATION

In the theoretical description of the second-harmonic generation we have neglected the depletion of the pump beams and have assumed that the beams are homogeneous. In the practical situation the pump depletion could be neglected but the beams are of finite sizes, so the walk off in long crystals will play an important role. Here we perform the numerical simulations of Eqs. (27). In practical situation the Gaussian Schell model [14] should be used. Then, the amplitude of the single beam can be written as

$$B_n(x,y) = b_0 \exp[-(x^2+y^2)/d^2] \times \sum_{s=1}^{N_s} \exp(iK_{xs}x + iK_{ys}y + i\xi_s), \tag{49}$$

where d is a beam envelope radius, K_{xs} and K_{ys} are the random number of normal distribution with variance $\Delta\beta/\sqrt{2}$, where $\Delta\beta = 2/\rho$, and ξ_s is a uniformly distributed phase. N_s has to be sufficiently large. The first fundamental beam consists of N of such Gaussian Schell-model beams, Eq. (1), and the second beam was constructed from N Gaussian beams of the same radius d. The phases of the beams were random. Equations (27) were simulated 50 times for a 1 cm long KTP crystal and the average values were fixed. The simulations were performed by the use of the symmetrized split-step Fourier method [15]. The results are presented in Figs. 4 and 5. The fundamental beams are depicted in Fig. 4. Good agreement between the numerical (Fig. 5) and the theoretical (Fig. 3) results was obtained.

V. CONCLUSIONS

In conclusion, we demonstrated the possibility to improve the coherence in the two-dimensional case. The spectrum of the second-harmonic beam narrows with the propagation in a nonlinear crystal when fundamental beams are two incoherent conical beams. One of these beams is radially coherent and the other is incoherent both radially and azimuthally. The simple interpretation of the result follows from the simplified experiment of two intersecting fundamental beams. In this case the width of the generated second-harmonic spectrum decreases in one direction. The spectrum is a line that can be rotated by changing the intersection plane. In the case of conical beams the line direction is undefined, so only the central component of the spectrum remains.

ACKNOWLEDGMENT

This work was supported by Research Council of Lithuania, Project No. MIP-073/2013.

[1] A. Picozzi and M. Haelterman, Phys. Rev. Lett. **86**, 2010 (2001).
[2] C. Montes, A. Picozzi, and K. Gallo, Opt. Commun. **237**, 437 (2004).
[3] S. Wabnitz, A. Picozzi, A. Tonello, D. Modotto, and G. Millot, JOSA B **29**, 3128 (2012).
[4] V. Pyragaite, A. Stabinis, A. Piskarskas, and V. Smilgevičius, Phys. Rev. A **87**, 063809 (2013).
[5] V. Pyragaite, V. Smilgevičius, R. Butkus, A. Stabinis, and A. Piskarskas, Phys. Rev. A **88**, 023820 (2013).
[6] A. Piskarskas, V. Pyragaite, and A. Stabinis, Phys. Rev. A **82**, 053817 (2010).
[7] A. Stabinis, V. Pyragaite, G. Tamošauskas, and A. Piskarskas, Phys. Rev. A **84**, 043813 (2011).
[8] V. Pyragaite, A. Stabinis, and A. Piskarskas, Phys. Rev. A **86**, 033812 (2012).
[9] J. Durnin, JOSA A **4**, 651 (1987).
[10] T. Wulle and S. Herminghaus, Phys. Rev. Lett. **70**, 1401 (1993).
[11] A. Piskarskas, V. Smilgevičius, A. Stabinis, and V. Vaičaitis, JOSA B **16**, 1566 (1999).
[12] I. S. Gradshteyn and I. M. Ryzhik, *Table of integrals, series, and products* (Academic Press, Waltham, Massachusetts, 2007).
[13] R. Gadonas, V. Jarutis, A. Marcinkevičius, V. Smilgevičius, and A. Stabinis, Opt. Commun. **167**, 299 (1999).
[14] G. Gbur, Opt. Express **14**, 7567 (2006).
[15] G. P. Agrawal, *Nonlinear fiber optics* (Academic Press, San Diego, 1989).